TISSUE ENGINEERING: Part A
Volume 24, Numbers 21 and 22, 2018

DOI: 10.1089/ten.tea.2017.0495

termis
Tissue Engineering
& Regenerative Medicine
International Society

ORIGINAL ARTICLE

Overcoming Challenges in Engineering Large, Scaffold-Free Neocartilage with Functional Properties

Brian J. Huang, PhD,[1,2] Wendy E. Brown, PhD,[3] Thomas Keown, BS,[4] Jerry C. Hu, PhD,[3] and Kyriacos A. Athanasiou, PhD, PE[3]

Although numerous cartilage engineering methods have been described, few report generation of constructs greater than 4 cm^2, which is the typical lesion size considered for cell-based therapies. Furthermore, current cell-based therapies only target focal lesions, while treatment of large nonisolated lesions remains an area of great demand. The objective of this study was to scale up fabrication of self-assembled neocartilage from standard sizes of 0.2 cm^2 to greater than 8 cm^2. Passaged sheep articular chondrocytes were self-assembled into 5 or 25-mm-diameter scaffoldless neocartilage constructs. The 25-mm-diameter constructs grew up to 9.3 cm^2 (areal scale-up of 23) and possessed properties similar to those of the 5-mm-diameter constructs; unfortunately, these large constructs were deformed and are unusable as a potential implant. A novel neocartilage fabrication strategy—employing mechanical confinement, a minute deadweight, and chemical stimulation (cytochalasin D, TGF-β1, chondroitinase-ABC, and lysyl oxidase-like 2 protein)—was found to successfully generate large (25-mm diameter) constructs with flat, homogeneous morphologies. Chemical stimulation increased collagen content and tensile Young's modulus 140% and 240% in the 25-mm-diameter constructs and 30% and 70% in the 5-mm-diameter constructs, respectively. This study not only demonstrated that exceedingly large self-assembled neocartilage can be generated with the appropriate combination of mechanical and chemical stimuli but also that its properties were maintained or even enhanced.

Keywords: large neocartilage, cartilage tissue engineering, cartilage repair, chondrocyte implantation, scaffold-free cartilage, biological scale-up

Introduction

Tissue engineering approaches have potential to overcome the shortcomings of clinically used cartilage repair options. In the Unites States, an estimated 250,000 articular cartilage repair procedures are performed annually.[1] Despite their prevalence, current repair therapies do not consistently fill the entire defect, and the repair tissue produced is not hyaline and does not integrate with the surrounding native tissue.

Microfracture has been shown to form a biomechanically inferior, fibrocartilaginous repair tissue, leading to repair tissue deterioration after 1.5–5 years.[2–5] Mosaicplasty with osteochondral autografts or allografts has been reported to fail in 15–55% of patients after 10 years.[6–8] Reasons include failure at the osseous region, poor lateral integration, and deterioration of graft edges. Autografts/allografts also have a limited supply source. Finally, results from autologous chondrocyte implantation (ACI) can be inconsistent; up to 85% of treated defects developed fibrocartilaginous fill.[9–11] These inconsistencies may arise from the uncontrolled placement of cells and an *in situ* neocartilage maturation process that is dependent on patient biology and postsurgery activities. To overcome these problems, tissue engineering strategies need to be developed so that engineered neocartilage constructs may be consistently engineered to have functional hyaline-like matrix and with anatomically relevant dimensions.

In a study investigating 25,000 knee arthroscopies, the majority of chondral lesions (70%) were shown to be nonisolated lesions (i.e., defined as having four or more focal lesions).[12] Treatment algorithms based on lesion size suggest the use of microfracture and osteochondral autografts for small focal lesions less than 2–2.5 cm^2.[8,13] Microfracture is generally indicated for small defects, as the biomechanically inferior repair tissue requires a border of native tissue

[1]Integrative Stem Cell Center, China Medical University Hospital, Taichung, Taiwan.
[2]Institute of New Drug Development, China Medical University, Taichung, Taiwan.
[3]Department of Biomedical Engineering, University of California Irvine, Irvine, California.
[4]School of Medicine, University of California Irvine, Irvine, California.

for mechanical support. The size of osteochondral autografts is limited to minimize donor site morbidity. Osteochondral allografts and ACI have been recommended to treat lesions greater than 2–2.5 cm^2 [8,13] and, on average, focal lesions of 4 cm^2.[14] Even tissue-engineered cartilage products currently in clinical trials, representing the next-generation therapies, limit their clinical indications to focal defects less than 7.5 cm^2.[15–24] Large, nonisolated defects generally receive palliative treatment until total or partial knee arthroplasty is indicated. Therefore, a tissue engineering approach that bridges the treatment of focal defects and total joint arthroplasty remains an unmet need for the foreseeable future. The next step in cartilage tissue engineering would involve fabricating constructs not only with functional properties but also of sufficient size to treat cartilage lesions of all sizes.

Engineered neocartilage with hyaline-like matrix composition and functional biomechanical properties has been fabricated using the self-assembling process.[25,26] In the self-assembling process, articular chondrocytes (ACs) are seeded at high density in nonadherent agarose wells.[27,28] Recently, passaged ACs were used as a cell source in fabricating these neocartilage constructs.[25,29,30] ACs underwent chondrotuning expansion[29] and aggregate redifferentiation to enhance redifferentiation of the dedifferentiated chondrocytes.[30,31] With these cells, it was shown that 2 million cells per 5-mm-diameter disc allowed the formation of homogeneous tissues with a hyaline-like matrix (abundant type II collagen; little to no type I collagen) and tensile properties near those of juvenile articular cartilage.[25]

A significant scale-up of the self-assembling process would be necessary to generate neocartilage constructs that can treat all types of articular lesions. Currently, most self-assembled neocartilage constructs may grow to at most 7 mm, or 0.4 cm^2 in area. Although diffusion in the axis of cartilage thickness may be similar in both the small and large constructs, radial diffusion will be severely limited when scaling up to large constructs, potentially adversely affecting construct biomechanical properties or matrix composition. Another challenge is maintaining shape fidelity when growing large neotissues. The logistics of creating a large construct, from chondrocyte passaging to mold fabrication, may also pose unforeseen challenges. Thus, scaling up the self-assembling process may not be a simple or straightforward process and should be investigated as a critical step in pushing the technology toward broad clinical application.

Application of chemical stimuli (cytochalasin D, TGF-β1, chondroitinase-ABC [C-ABC], and lysyl oxidase like 2 [LOXL2] protein), which had been originally developed in 5-mm-diameter self-assembled neocartilage constructs, may not necessarily induce the same effects in scaled-up constructs because of diffusion limitations or other unforeseen variables. TGF-β1 is an anabolic factor known to promote chondrogenesis and enhance glycosaminoglycan (GAG) and type II collagen synthesis.[32,33] C-ABC acts by temporarily depleting GAGs in the constructs, restructuring the matrix to allow the development of a matrix richer in collagens and allowing formation of thicker collagen fibers.[34] LOXL2 was not shown to affect neocartilage matrix content, but was able to increase tissue tensile properties by increasing the number of pyridinoline collagen crosslinks.[26] Cytochalasin D, a potent inhibitor of intracellular actin stress fiber formation, has been shown to induce a rounded cell phenotype and chondrogenesis in stem cells.[35] Although these chemical stimuli have been shown to enhance neocartilage properties in ''small'' constructs, whether they can enhance properties in ''large'' constructs is an important criterion in successfully scaling up the self-assembling process.

Young ACs have a superior capability to secrete cartilage matrix molecules compared to adult chondrocytes or stem cells that have been expanded.[36] Young chondrocytes also have significantly higher collagen II gene expression[36,37] and drastically higher GAG production than adult chondrocytes.[36,38] A cell source capable of maintaining its chondrogenic phenotype after expansion will be critical for the generation of functional cartilage. Allogeneic chondrocytes have also been shown to be nonimmunogenic.[39] Currently, young allogeneic ACs have been approved for use in cartilage repair in the form of particulated allografts (i.e., DeNovo® NT by Zimmer). The same cell source is used by a tissue-engineered cartilage product (i.e., RevaFlex™) currently in Phase III clinical trials. These examples demonstrate clinical feasibility of applying young, allogeneic cells for cartilage repair.

The objective of this study was to scale up self-assembled neocartilage from 0.2 cm^2 to greater than 8 cm^2 without compromising the constructs' functional properties or their response to beneficial chemical stimulation treatment (i.e., cytochalasin D, TGF-β1, C-ABC, and LOXL2). The hypothesis was that there would be no difference in the functional properties between the established model of self-assembled neocartilage formation (i.e., 5-mm-diameter constructs) and a significantly scaled-up version (i.e., 25-mm-diameter constructs). Constructs of both diameters were formed with or without chemical stimulation, and, at the end of 6 weeks of culture, constructs were evaluated grossly, biochemically, and mechanically. Scaling up the self-assembling process to such a size would enable its broad use in cartilage repair by treating a large range of lesion sizes.

Materials and Methods

Chondrogenic medium formulation

The chondrogenic medium used throughout the study comprised Dulbecco's modified Eagle medium (25 mM glucose/GlutaMAX™; Thermo Fisher Scientific, Waltham, MA), 1% (v/v) penicillin-streptomycin-amphotericin B (Lonza, Basel, Switzerland), 1% (v/v) insulin-transferrin-sodium selenite (BD Biosciences, San Jose, CA), 1% (v/v) NEAA (Thermo Fisher Scientific), 100 μg/mL sodium pyruvate (Thermo Fischer Scientific), 50 μg/mL ascorbate-2-phosphate (Sigma, St. Louis, MO), 40 μg/mL L-proline (Sigma), and 100 nM dexamethasone (Sigma).

Isolation of fetal sheep ACs

Fetal sheep ACs were isolated from the femoral condyle and trochlear groove of the knees of Dorper cross sheep in 120–125 day gestation (UC Davis School of Veterinary Medicine). Cartilage was minced into 1 mm^3 cubes and was washed with phosphate-buffered saline (PBS) before undergoing digestion with 500 units/mL collagenase type 2 (Worthington Biochemical, Lakewood, NJ) in chondrogenic

medium +3% (v/v) fetal bovine serum (FBS) (Atlanta Biologicals, Lawrenceville, GA) for 18 h at 37°C and 10% CO_2. Cells were then strained through a 70 μm filter, washed with red blood cell lysis buffer (154.4 mM ammonium chloride, 10 mM sodium bicarbonate, and 50 mM EDTA tetrasodium salt in ultrapure water) for 3 min, counted, and frozen in chondrogenic medium containing 20% (v/v) FBS +10% (v/v) DMSO (Sigma).

Chondrocyte passaging

Primary ACs underwent chondrotuning expansion in monolayer to passage 4 (P4), as previously described,[29] with some modifications. Briefly, P0 ACs were thawed and seeded into T225 flasks at ~25,000 cells/cm^2. For the first 24 h of each passage, 10% (v/v) FBS was added to the medium to promote cell adhesion. The concentration of FBS was then lowered to 3% (v/v) for the rest of the passage duration. Throughout culture, the medium was supplemented with 1 ng/mL TGF-β1, 5 ng/mL FGF-2, and 10 ng/mL platelet-derived growth factor BB (Peprotech, Rocky Hill, NJ), also known as TFP growth factor cocktail. The medium was changed every 3–4 days. All cultures took place at 37°C and 10% CO_2. Cells were grown an additional 4 days past 95% confluence. During passaging, cells were lifted with an incubation in 0.25% trypsin/EDTA (Invitrogen) for 20 min. The resulting cell solution was then digested with 500 units/mL collagenase in chondrogenic medium +3% (v/v) FBS for 45–60 min. Cells were filtered through a 70 μm cell strainer, washed thrice, counted with a hemocytometer, and either passaged again into monolayer (as described above) or into aggregate culture, as described next.

Aggregate culture

Passaged ACs underwent aggregate redifferentiation, as previously described.[30,31] Briefly, 10 cm petri dishes were first coated with a thin layer of 2% molten agarose to prevent cell adhesion. In each dish, 25 million cells were placed in 25 mL chondrogenic medium supplemented with 10 ng/mL TGF-β1, 100 ng/mL BMP-2, and 100 ng/mL GDF-5 (Peprotech). Dishes were put on an orbital shaker at 55 rpm for 24 h and then cultured statically for an additional 13 days. Medium was changed every 2–3 days. At day 14, cell aggregates were digested with 0.25% trypsin/EDTA for 20 min, the trypsin removed, and then digested in 500 units/mL collagenase in chondrogenic medium +3% FBS for 90–120 min. Cells were filtered through a 70 μm cell strainer, washed thrice, counted, and used for the self-assembly of neocartilage constructs.

Self-assembly of neocartilage constructs

Scaffold-free neocartilage constructs, formed by the self-assembling process,[27] were generated by seeding ACs into 2% agarose wells with an inner diameter of 5 or 25 mm. Custom-machined, 5-mm-diameter stainless steel posts were used as negative casts to create agarose self-assembly wells in 750 μL of 2% agarose in each well within a 48-well plate. Agarose wells, 25 mm in diameter, were also created using a mold system consisting of 3D printed parts (printed with an Objet system using MED610 or Vero White materials; Stratasys, Eden Prairie, MN). All agarose wells were saturated with several changes of chondrogenic medium for 5 days before cell seeding.

To form 5-mm-diameter neocartilage constructs, 2 million cells in 80 μL chondrogenic medium were seeded into empty 5-mm-diameter agarose wells. After a 4-h incubation, 500 μL medium was carefully added to each well so as to not disturb the nascent construct ($t = 0$ days). Every 24 h, 500 μL medium was changed. At day 2, constructs were unconfined and placed into 10.5-mm-diameter, 2% agarose wells (formed by using 3D printed pegs as a negative cast) in 24-well plates. Every 48 h, 1 mL of medium was changed. At day 4, an agarose disc (10-mm diameter by 2-mm thick, formed by a mold system consisting of 3D printed parts) was added to the top of each construct, followed by addition of an 8-mm-diameter, 7 mg plastic deadweight (taking into account buoyancy in water; printed with MED610). The deadweight was only applied every other day until day 21 and from days 28–35.

To form 25-mm-diameter constructs, 50 million cells in 2 mL medium were seeded into empty 25-mm-diameter agarose wells placed on top of 3D printed plastic stands (Fig. 1A). The agarose wells and stands were housed in 10-cm-diameter, 2.5-cm-tall petri dishes. The plastic stands served to enhance nutrient diffusion. After a 4-h incubation, 2 mL medium was carefully added to cover the agarose well. A 3D printed plastic weight was placed on top of the agarose well to prevent it from excessively moving during handling. At day 2, constructs were unconfined and placed into 35-mm-diameter, 2% agarose wells (formed by using a mold system of 3D printed parts) in petri dishes. It was known that constructs would begin developing a curled morphology (Fig. 1B). To maintain a flat morphology, at day 4, a 33-mm-diameter, 2.5-mm-thick agarose disc (formed by a mold system consisting of 3D printed parts) was added to the top of each construct, followed by addition of a 30-mm-diameter, 175 mg plastic deadweight (taking into account buoyancy in water; printed with MED610; Fig. 1C). The deadweight was applied at the same temporal regimen as for the 5-mm constructs. Every 5–6 days, 60 mL of medium was changed.

After 42 days, constructs were photographed and their wet weights (WW) were recorded. Each construct was then assayed by histology, and biochemical and biomechanical assays.

Chemical stimulation treatment

For groups subjected to chemical stimulation treatment, 2 μM cytochalasin D (Enzo Life Sciences, Farmingdale, NY) was supplemented to the medium at days 0–3; 10 ng/mL TGF-β1 was supplemented throughout culture (days 0–42); and LOXL2 cocktail was supplemented at days 21–42 (LOXL2 cocktail consisted of 0.15 μg/mL lysyl oxidase-like 2 (LOXL2). Protein (Genway Bio, San Diego, CA) +1.6 μg/mL copper sulfate (Sigma) +146 μg/mL hydroxylysine [Sigma]); and 2 U/mL chondroitinase ABC (C-ABC; Sigma), activated with 0.05 M sodium acetate (Sigma), were applied for 4 h at day 21 (Fig. 1D). After C-ABC application, constructs were washed with chondrogenic medium containing 1 mM zinc sulfate (Sigma) thrice to deactivate and remove residual C-ABC.

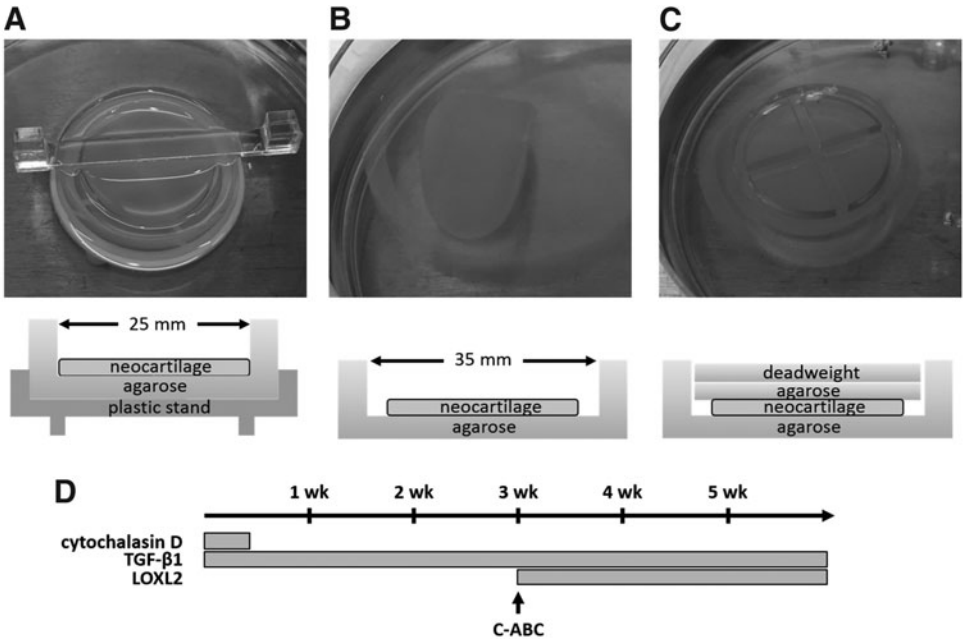

FIG. 1. Experimental timeline and setup during neocartilage culture. **(A)** At day 0, passage 4 chondrocytes in chondrogenic medium + TGF-β1 + cytochalasin D were seeded into 25-mm-diameter agarose wells on top of plastic stands. The stands allowed for better nutrient diffusion. After 4 h, during which the chondrocytes self-assembled and formed a solid construct, culture medium (chondrogenic medium + TGF-β1 + cytochalasin D) was added to the petri dish to cover the entire agarose well. Plastic well weights acted to prevent movement of the well during handling. At day 2, neocartilage constructs were unconfined and transferred to 35-mm agarose wells (without a plastic stand). At day 3, cytochalasin D treatment was stopped by switching the medium to chondrogenic medium + TGF-β1. **(B, C)** At day 4, neocartilage constructs were observed to exhibit curling; an agarose disc and a deadweight were added for the purpose of maintaining a flat construct morphology. **(D)** Timeline of chemical stimulation application: cytochalasin D was applied from day 0–3; TGFβ-1 was applied throughout culture; LOXL2 cocktail (LOXL2 + hydroxylysine + copper sulfate) was applied from day 21–42; C-ABC was applied for 4 h at day 21. Generation of 5-mm constructs followed similar protocols. C-ABC, chondroitinase-ABC; LOXL2, lysyl oxidase like 2.

Histology and immunohistochemistry

Tissue samples ($\sim 1 \times 1 \times 1$ mm) were embedded in Histo-Prep (Thermo Fisher Scientific) and cryosectioned to 16-μm-thick sections, and mounted on glass slides. Staining for GAGs was performed with Safranin O, Fast Green, and Weigert's hematoxylin. Collagen staining was performed with Picrosirius Red. Collagen I and II immunohistochemistry were also performed, as described previously.[40] Color was developed using the Vectastain ABC reagents and DAB (Vectastain).

Biochemical analysis

Neocartilage samples, $\sim 3 \times 1 \times 1$ mm ($\sim$5–12 mg), were weighed to obtain WW, lyophilized for 3 days, and weighed again to obtain dry weights. Samples were digested in digest solution consisting of 125 μg/mL papain +5 mM N-acetyl-L-cysteine +5 mM EDTA in phosphate buffer, pH 6.5.

Total collagen content was measured using a modified chloramine-T colorimetric assay for hydroxyproline content.[41] For each sample, 100 μL of the digested engineered construct was added to 100 μL 1 × tris-buffered saline, hydrolyzed with 200 μL 4 N NaOH at 120°C for 15 min in an autoclave, and then neutralized with 200 μL 4 N HCl. Samples were then incubated with 1.25 mL of 0.062 M chloramine T (Sigma) in an acetate-citrate buffer (0.45 M NaOH, 0.45 M sodium acetate, 0.14 M citric acid, and 0.11 M acetic acid), for 20 min at room temperature. Samples were then incubated with 1.25 mL of 1.2 M Ehrlich's reagent (Sigma) in 30% perchloric acid +70% isopropanol for a 20-min incubation at 65°C for color development. Samples were plated in duplicates and absorbance measured at 550 nm with a microplate reader. Equal amounts of digest solution were been added to the standards (bovine collagen from the Sircol Collagen Assay; Biocolor, Carrickfergus, United Kingdom) and samples to ensure consistency.

Total sulfated GAG content was measured using the Blyscan GAG assay kit (Biocolor) following the manufacturer's instructions. Briefly, 10 μL of digested sample was incubated with 500 μL dye reagent for 30 min, vortexing periodically. The samples were centrifuged to precipitate of the bound dye, and the pellet was dissolved in 500 μL dissociated reagent. Solutions were plated to microplates and absorbance measured at 650 nm. DNA content was assessed with the Picogreen assay. Briefly, 10 μL of the digested sample was added to each well along with the Picogreen reagents; fluorescence was measured at 485/528 nm Ex/Em.

Biomechanical analysis

For tensile testing, dog bone-shaped samples were cut from each engineered construct. The dog bone samples were then photographed and glued to paper tabs with a gauge length of 1.27 mm, and underwent uniaxial tension using an Instron model 5565 (Instron, Canton, MA).[42] A strain rate of 1% the gauge length/s was used. Sample cross-sectional areas were

calculated in ImageJ from high-resolution photographs of the dog bone. The Young's modulus was obtained from the linear region of the stress-strain curve and the ultimate tensile strength (UTS) was defined as the maximum stress obtained.

For compressive testing, a 3-mm-diameter sample was taken from the middle of each engineered construct with a biopsy punch. The sample was placed in a PBS bath at room temperature and underwent unconfined stress-relaxation, as described previously.[43] Sample heights were determined by lowering the platen until a load change of 0.02 N was detected. Samples were then compressed to 10% strain at a rate of 1% the sample height/s, held for 200 s, compressed to 20% strain, and held for 450 s. The instantaneous and relaxation moduli of the 20% strain curve were determined by using a curve fit and the standard linear solid, finite deformation model[43] using MatLab software.

Statistics

All results were analyzed with a one-factor ANOVA and Tukey's *post hoc* test ($p < 0.05$) using JMP 10 software (SAS Institute). Data are presented as means, and error bars represent standard deviations among biological replicates within the same group. A sample size of $n = 6–8$ per group was used. Significant differences are indicated by different letters by each value.

Results

Neocartilage gross morphology

The gross morphological properties of the self-assembled neocartilage constructs after 6 weeks of culture are presented in Figure 2. The 5-mm control constructs developed bowl-shaped morphologies, as previously observed,[25] while the 5-mm stimulated constructs had flat morphologies. The 25-mm control constructs exhibited morphological deformities such as wrinkles and pockets of fluid-filled cavities, while the 25-mm stimulated constructs were flat, homogeneous, and solid. The 5-mm control, 5-mm stimulated, 25-mm control, and 25-mm stimulated constructs grew to an average of 7, 8, 34, and 32 mm in diameter. The thicknesses of all constructs were generally slightly less than 1 mm. Chemical stimulation reduced the thickness of both 5-mm and 25-mm constructs, although only significantly so for the 25-mm constructs. Regional analysis of the 25-mm constructs showed significantly thicker edges than the center.

Histology and immunohistochemistry

Saf-O/Fast Green and Picrosirius Red staining revealed the abundant presence of GAGs and collagen, respectively, throughout the neocartilage constructs (Fig. 3). Differences in staining intensity and staining distribution were not observed among any groups. Immunohistochemistry revealed presence of type II collagen throughout all constructs. Collagen I immunohistochemical staining revealed only trace amounts of collagen type I. Histological characteristics qualitatively support the formation of hyaline-like cartilage in all constructs.

Neocartilage biochemical properties

Collagen content, as measured by collagen per WW (collagen/WW), was not different between the unstimulated 5-mm and unstimulated 25-mm constructs (Fig. 4). It should be noted

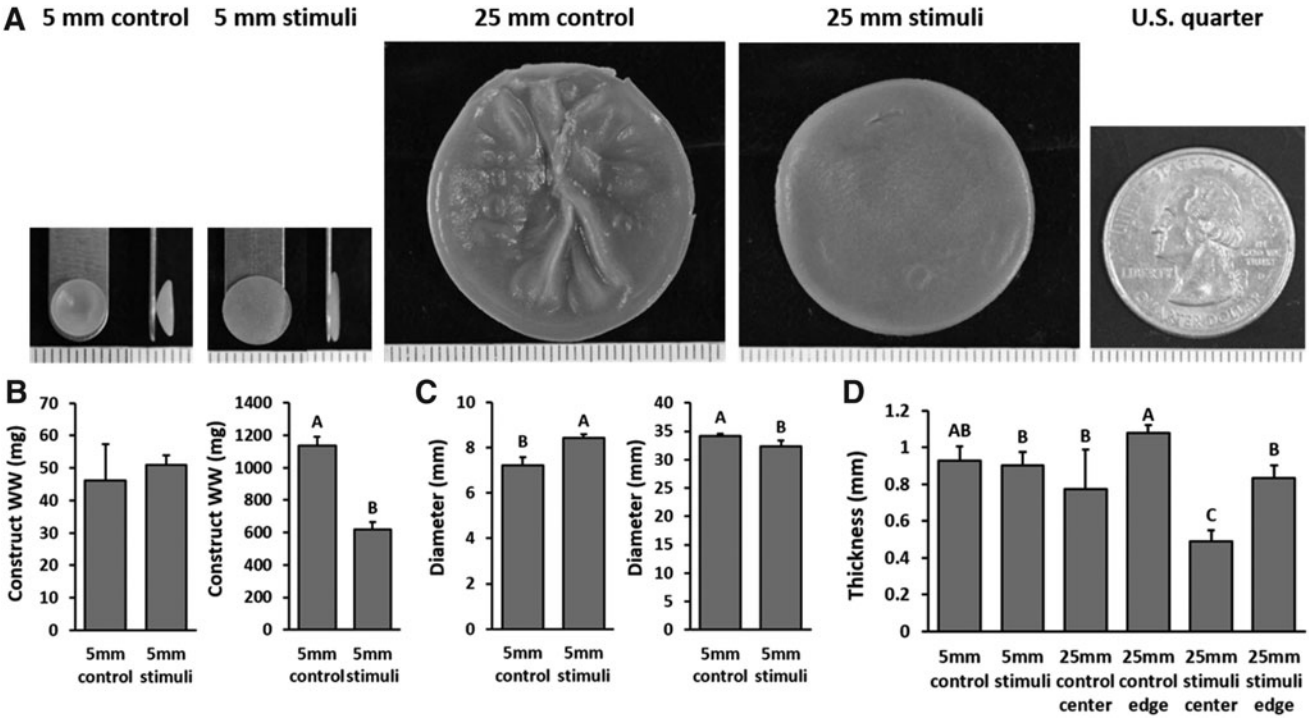

FIG. 2. Gross morphology images and growth metrics of the 5- and 25-mm-diameter constructs at the end of 6 weeks of culture. Front and side images of the 5-mm-diameter constructs, front images of the 25-mm-diameter constructs, and an image of a U.S. quarter for comparison **(A)**. Each tick mark on the ruler represents 1 mm. WW **(B)**, diameter **(C)**, and thickness **(D)** of the constructs. WW, wet weight.

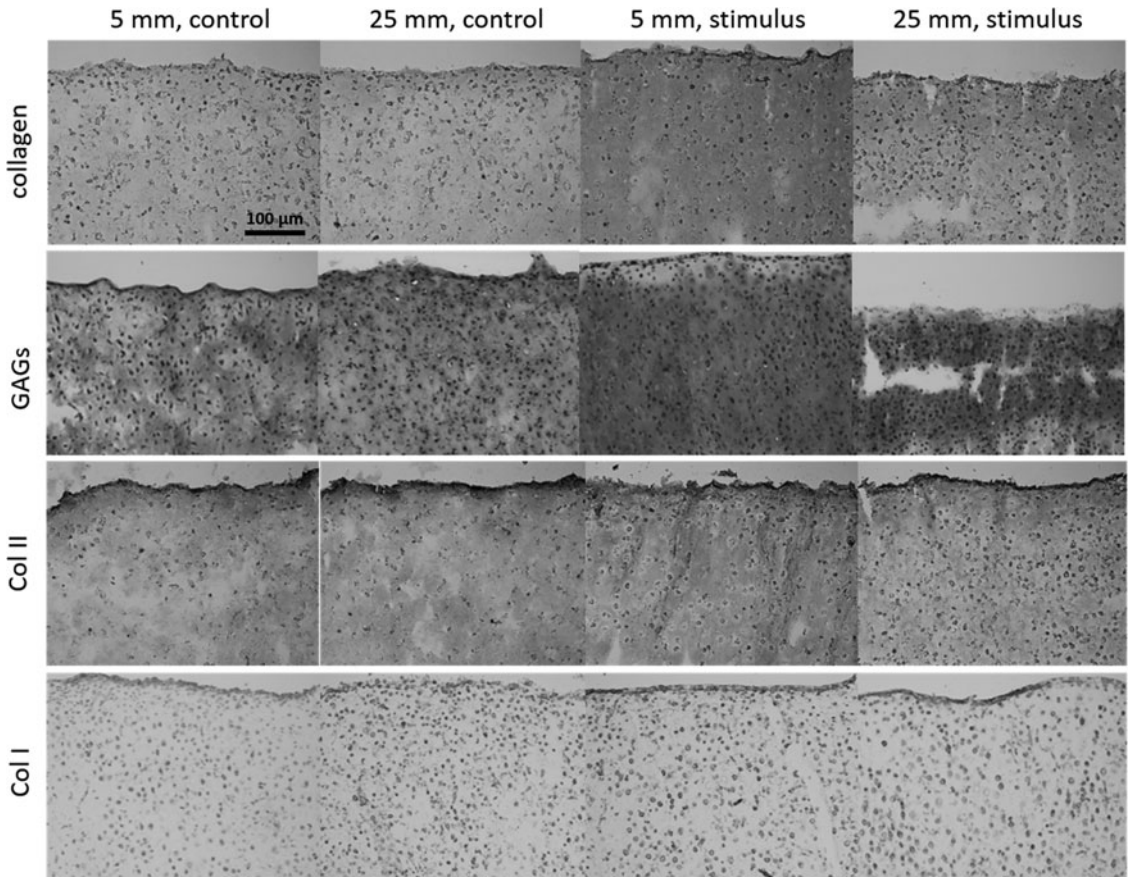

FIG. 3. Histological analysis indicates that neocartilage constructs have a matrix rich in collagen, as stained by Picrosirius Red, and GAGs, as stained by Saf-O/Fast Green. Immunohistochemistry stains show presence of type II collagen in all constructs with little to no type I collagen. GAG, glycosaminoglycan.

that for this figure, the values of the 25-mm-diameter constructs represent the average values of samples from both the center and edge regions. No difference was observed between the stimulated 5-mm and stimulated 25-mm constructs. Chemical stimulation increased collagen/WW in both the 5-mm and 25-mm constructs, but only significantly so in the 25-mm constructs (140% increase). Collagen/WW of the edge and center of the large constructs was similar.

GAG content, as measured by GAG/WW, was largely unchanged between the 5-mm and 25-mm constructs in both the control and stimulated groups. Applied chemical stimulation slightly increased but did not significantly change the GAG content of neocartilage constructs. GAG/WW of the edge and center of the large constructs was similar.

Cellularity of the constructs, as measured by DNA/WW, was not significantly different among all groups. Water content, an inverse measure of the general density of the tissue extracellular matrix, was significantly decreased by chemical stimulation in both the 5-mm- and 25-mm-diameter constructs, indicating that stimulation was able to consistently increase the solid tissue density in neocartilage.

Neocartilage biomechanical properties

The tensile properties, as measured by the Young's modulus and the UTS, were not different between the unstimulated 5-mm and unstimulated 25-mm constructs (Fig. 5). Interestingly, chemical stimulation increased the tensile properties of the 25-mm constructs (240% increase in Young's modulus and 500% increase in UTS) more compared with the 5-mm constructs (70% increase in Young's modulus and 140% increase in UTS). This led to the 25-mm-stimulated constructs having significantly higher tensile properties compared with the 5-mm-stimulated constructs. The center region of the 25-mm-stimulated constructs had a higher Young's modulus than the edge regions, although this trend was not seen in the UTS values.

The compressive properties, as measured by the instantaneous modulus and relaxation modulus, were not different between the unstimulated 5-mm and unstimulated 25-mm constructs. No difference was also observed between the stimulated 5-mm and stimulated 25-mm constructs. Chemical stimulation significantly increased the instantaneous modulus of the 5-mm constructs, but did not affect relaxation modulus in either the 5-mm or 25-mm constructs. The compressive properties of the edge and center regions of the large constructs remained largely similar; however, the center of the 25-mm-stimulated constructs had higher instantaneous modulus values than its edge.

Discussion

Toward addressing the current need to repair large or nonisolated cartilage defects, which represent the majority

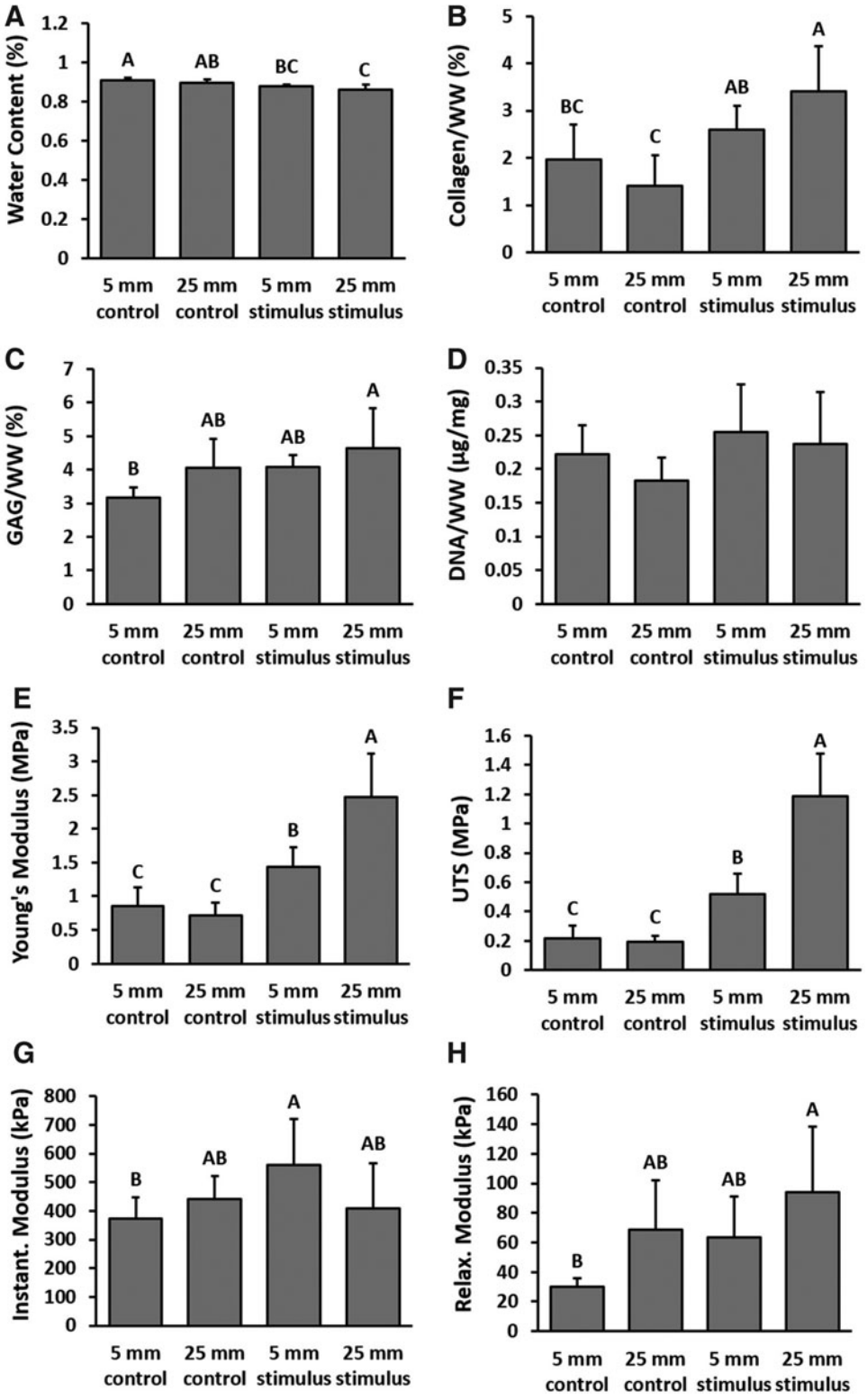

FIG. 4. Biochemical and biomechanical properties of 5-mm-diameter constructs compared to 25-mm-diameter constructs at the end of 6 weeks of culture. One sample per 5-mm-diameter construct was evaluated. For 25-mm-diameter constructs, one edge and one center sample were pooled per construct. Water content **(A)**, collagen/WW **(B)**, GAG/WW **(C)**, DNA/WW **(D)**, tensile Young's modulus **(E)**, tensile UTS **(F)**, compressive instantaneous modulus **(G)**, and compressive relaxation modulus **(H)** are presented. Different letters denote statistical significance ($p < 0.05$) amongst groups. UTS, ultimate tensile strength.

of lesions in patients, the objectives of the study were: (1) to fabricate scaffold-free neocartilage greater than 8 cm^2 by scaling up the self-assembling process and 2) to determine whether the scale-up process would adversely affect neocartilage properties or response to a regimen of chemical stimuli (cytochalasin D, TGF-β1, LOXL2, and C-ABC). The hypothesis was that neocartilage properties would not be compromised through the scale-up process and that the chemical stimuli would retain their beneficial effects. Analysis of construct matrix content and biomechanics supports that the 25-mm-diameter constructs, which grew up to 9.3 cm^2, possessed functional properties on par with the small (0.4 cm^2) constructs. The largest constructs generated in the study represented a scale-up factor of 23-fold over the

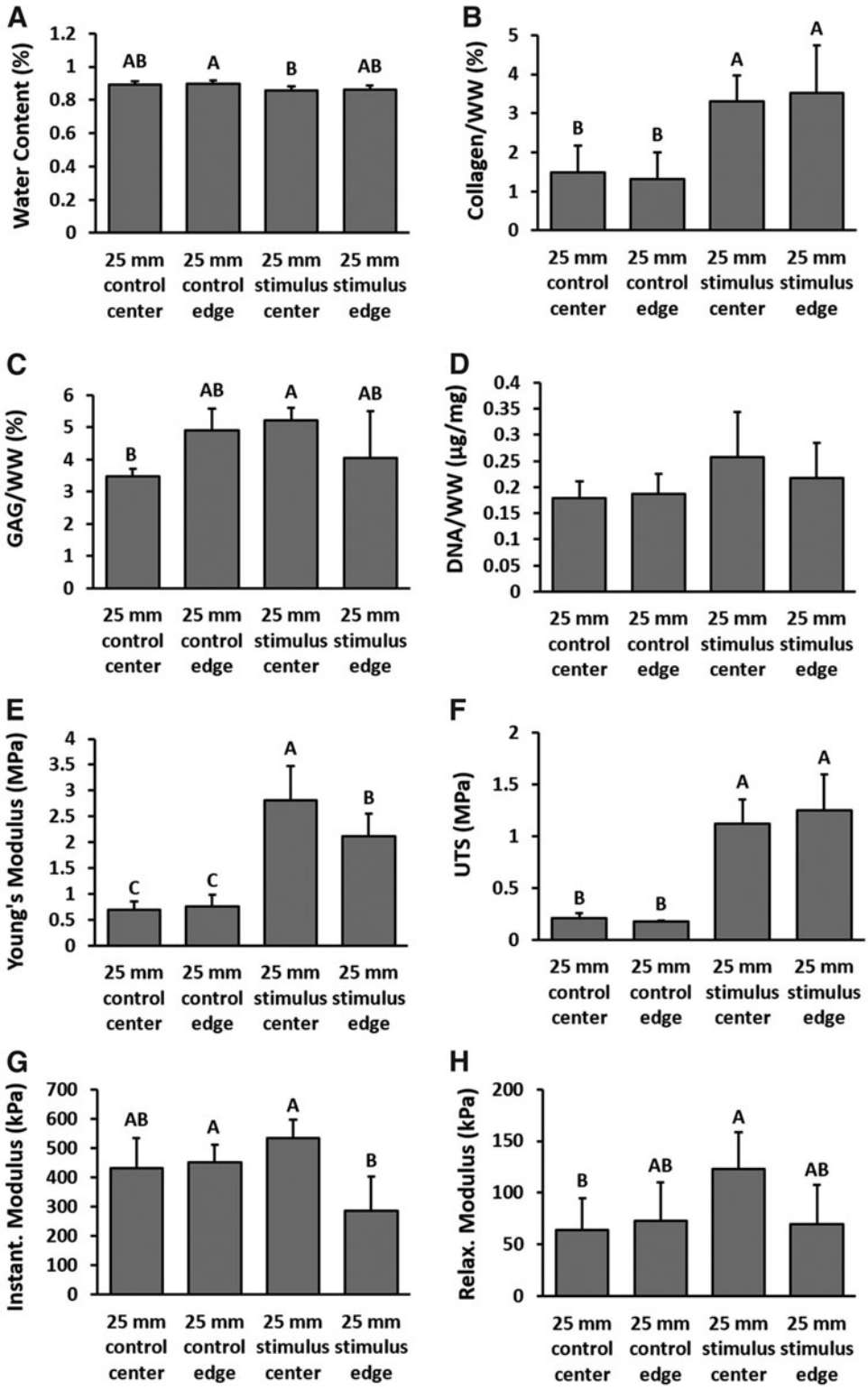

FIG. 5. Biochemical and biomechanical properties of the center region compared to the edge region of 25-mm-diameter constructs at the end of 6 weeks of culture, as characterized by water content **(A)**, collagen/WW **(B)**, GAG/WW **(C)**, DNA/WW **(D)**, tensile Young's modulus **(E)**, tensile UTS **(F)**, compressive instantaneous modulus **(G)**, and compressive relaxation modulus **(H)**. Different letters denote statistical significance ($p < 0.05$) amongst groups.

small constructs. However, without chemical stimuli, large constructs contained folds and pockets of fluid-filled cavities, indicating that scale-up of engineered tissues remains a challenging and nonstraightforward process.[44] Through novel fabrication protocols and application of chemical stimulation, this study demonstrated that the 25-mm-diameter constructs can be made into uniformly flat, homogeneously solid neotissues, possessing properties on par with or even higher than those of the standard 5-mm-diameter constructs. Specifically, chemical stimulation was shown to increase tensile Young's modulus, UTS, and collagen/WW in the stimulated 5-mm-diameter constructs by 70%, 140%, and 30% over unstimulated controls; in the 25-mm-diameter constructs, these properties were increased even further—240%, 510%,

and 140%—over controls. This study showed that significant scale-up of the self-assembling process is possible and that neocartilage functional properties can be maintained or even enhanced in the process. Fabrication of large functional neocartilage provides a key step toward potentially treating large or nonisolated lesions, bridging the gap between current repair therapies and knee arthroplasty, and pushing cartilage tissue engineering toward new possibilities.

This study represented the culmination of a series of pilot studies with the intent to induce a flat and homogeneous morphology in the 25-mm-diameter constructs. This was achieved by three key processes: (1) application of chemical stimulation, (2) unconfinement at an early time point (day 2), and (3) application of a light deadweight at day 4. The key component within the chemical stimulation treatment that helped prevent formation of folds and fluid-filled cavities present in the control constructs was cytochalasin D. Without cytochalasin D, control constructs were observed to start forming folds within 24 h. Application of cytochalasin D was observed to mitigate or delay this phenomenon until day 2. Cytochalasin D has been shown to inhibit the formation of actin stress fibers within cells, thus inducing a rounded cell morphology and inhibiting cell migration. The formation of internal stresses by actin stress fiber contraction may lead to the development of these folds within the constructs in this study. The previously reported chondrogenesis-inducing capabilities of cytochalasin D[35,45] may also play a role encouraging a chondrogenic phenotype in the passaged cells used within this study, resulting in more robust neocartilage. At day 2, folds start to appear even in the presence of cytochalasin D, possibly due to lateral expansion of the construct as cells begin secreting an abundance of extracellular matrix. To mitigate the development of folds, the constructs were carefully unconfined at day 2 (the earliest time point in which these constructs can be handled without introducing tears) and transferred to larger 35-mm-diameter agarose wells. At day 4, large constructs were observed to begin curling, indicating the formation of internal stresses within the construct. These stresses could arise for several reasons, such as incomplete redifferentiation of chondrocytes, tightening of the contiguous matrix, or formation of stronger cell-matrix interactions during neocartilage formation. Such phenomena need to be elucidated in further studies. Nevertheless, to maintain a flat morphology, the constructs were axially confined at day 4 with the addition of an agarose disc and an exceedingly light deadweight (175 mg, taking into account the buoyancy of the plastic in fluid). In pilot experiments, heavier weights induced construct disintegration, as the constructs were still mechanically weak at day 4. Furthermore, to minimize potential obstruction of neocartilage growth by the deadweight, it was removed periodically as specified in the methods. The introduction of these steps to an already established protocol of generating self-assembled neocartilage, along with chemical stimulation, helped generate a flat and homogeneous morphology in the large, self-assembled neocartilage constructs.

Due to their size, regional analysis was possible for the 25-mm-diameter constructs, while such analysis was not possible for the 5-mm-diameter constructs. Although the properties of the center and edge region of the large constructs were largely similar, some properties were different. Specifically, the center region was significantly thinner and exhibited significantly higher tensile Young's modulus and compressive instantaneous modulus than the edge region. Greater nutrient diffusion and access to the molecules that compose the chemical stimulation regimen may have allowed this region to develop better properties than the slightly thicker edges, or the 5-mm-diameter constructs overall. Previous attempts to generate large engineered cartilage constructs have also noted differences in properties between the edge and center. Large agarose-embedded chondrocyte constructs (1.5×1.5 cm and 2.5-mm thick), after 4 weeks of culture, were observed visually and histologically to have an edge region containing denser matrix than the center.[44] However, quantitative biochemical or biomechanical properties of these two regions were not compared. Large constructs (20–25 cm in diameter and 2.25-mm thick) in the shape of the femoral head of juvenile minipigs, composed of chondrocytes embedded in methacrylate-modified hyaluronic acid hydrogels, also exhibited edge effects.[46] After 12 weeks of culture, the center of the constructs had significantly lower collagen and GAG content and mechanical properties than the edges. The difference was attributed to potential diffusion limitations. In this study, the center of the constructs did not have inferior properties compared to those of the edge regions. Overall, the fabrication protocols described in this study allowed formation of large constructs with properties similar to those of the small constructs.

This study demonstrated the feasibility of generating functional neocartilage greater than 8 cm^2 without compromising its properties. These constructs can potentially be used to treat a broader range of cartilage lesion sizes compared to current therapies. Among current cartilage repair options, microfracture or osteochondral autografts have been stated to optimally treat lesions less than 2–2.5 cm^2 in area.[8,13] Above this size, cell-based therapies, such as ACI, tissue-engineered products, and osteochondral allografts, have been used to treat focal defects that are generally less than 7.5 cm^2 [14–24]; the average size of lesions treated by ACI and osteochondral allografts is 4 cm^2.[14] However, 70% of cartilage lesions have been shown to be nonisolated lesions,[12] which often exceed sizes larger than 7.5 cm^2. The large constructs generated in this study did not exhibit significant decreases in biochemical or functional biomechanical properties; in fact, some properties were enhanced during scale-up. With the current demonstration that such large neocartilage constructs can be fabricated, the next developmental phase would be to create anatomically correct morphologies. Functional neocartilage of these sizes can potentially treat large or nonisolated lesions. Repair therapy using these scaled-up constructs can potentially bridge the gap between current therapies that only treat focal defects and total or partial knee arthroplasty.

Acknowledgments

We gratefully acknowledge NIH grant no. R01AR067821 for partially funding this work.

Disclosure Statement

No competing financial interests exist.

References

1. McCormick, F., Harris, J.D., Abrams, G.D., *et al.* Trends in the surgical treatment of articular cartilage lesions in the United States: an analysis of a large private-payer database over a period of 8 years. Arthroscopy **30,** 222, 2014.
2. Kreuz, P.C., Steinwachs, M.R., Erggelet, C., *et al.* Results after microfracture of full-thickness chondral defects in different compartments in the knee. Osteoarthritis Cartilage **14,** 1119, 2006.
3. Gobbi, A., Karnatzikos, G., and Kumar, A. Long-term results after microfracture treatment for full-thickness knee chondral lesions in athletes. Knee Surg Sports Traumatol Arthrosc **22,** 1986, 2014.
4. Goyal, D., Keyhani, S., Lee, E.H., and Hui, J.H. Evidence-based status of microfracture technique: a systematic review of level I and II studies. Arthrosc J Arthrosc Relat Surg Off Publ Arthrosc Assoc North Am Int Arthrosc Assoc **29,** 1579, 2013.
5. Mithoefer, K., McAdams, T., Williams, R.J., Kreuz, P.C., and Mandelbaum, B.R. Clinical efficacy of the microfracture technique for articular cartilage repair in the knee: an evidence-based systematic analysis. Am J Sports Med **37,** 2053, 2009.
6. Bentley, G., Biant, L.C., Vijayan, S., Macmull, S., Skinner, J.A., and Carrington, R.W. Minimum ten-year results of a prospective randomised study of autologous chondrocyte implantation versus mosaicplasty for symptomatic articular cartilage lesions of the knee. J Bone Joint Surg Br **94,** 504, 2012.
7. Gross, A.E., Kim, W., Las Heras, F., Backstein, D., Safir, O., and Pritzker, K.P. Fresh osteochondral allografts for posttraumatic knee defects: long-term followup. Clin Orthop Relat Res **466,** 1863, 2008.
8. Demange, M., and Gomoll, A.H. The use of osteochondral allografts in the management of cartilage defects. Curr Rev Musculoskelet Med **5,** 229, 2012.
9. Bartlett, W., Skinner, J.A., Gooding, C.R., *et al.* Autologous chondrocyte implantation versus matrix-induced autologous chondrocyte implantation for osteochondral defects of the knee: a prospective, randomised study. J Bone Joint Surg Br **87,** 640, 2005.
10. Shekkeris, A., Perera, J., Bentley, G., *et al.* Histological results of 406 biopsies following ACI/MACI procedures for osteochondral defects in the knee. J Bone Joint Surg Br **94-B(Suppl. XXXVI),** 12, 2012.
11. Ringe, J., Burmester, G.R., and Sittinger, M. Regenerative medicine in rheumatic disease-progress in tissue engineering. Nat Rev Rheumatol **8,** 493, 2012.
12. Widuchowski, W., Widuchowski, J., and Trzaska, T. Articular cartilage defects: study of 25,124 knee arthroscopies. Knee **14,** 177, 2007.
13. Schindler, O.S. (iv) Articular cartilage surgery in the knee. Orthop Trauma **24,** 107, 2010.
14. Behrens, P., Bitter, T., Kurz, B., and Russlies, M. Matrix-associated autologous chondrocyte transplantation/implantation (MACT/MACI)–5-year follow-up. Knee **13,** 194, 2006.
15. Elder, B.D., Kim, D.H., and Athanasiou, K.A. Developing an articular cartilage decellularization process toward facet joint cartilage replacement. Neurosurgery **66,** 722, 2010.
16. Ofek, G., Natoli, R.M., and Athanasiou, K.A. In situ mechanical properties of the chondrocyte cytoplasm and nucleus. J Biomech **42,** 873, 2009.
17. Boyle, J., Luan, B., Cruz, T.F., and Kandel, R.A. Characterization of proteoglycan accumulation during formation of cartilagenous tissue in vitro. Osteoarthritis Cartilage **3,** 117, 1995.
18. Furukawa, K.S., Suenaga, H., Toita, K., *et al.* Rapid and large-scale formation of chondrocyte aggregates by rotational culture. Cell Transplant **12,** 475, 2003.
19. Elloumi-Hannachi, I., Yamato, M., and Okano, T. Cell sheet engineering: a unique nanotechnology for scaffold-free tissue reconstruction with clinical applications in regenerative medicine. J Intern Med **267,** 54, 2010.
20. Mori, Y., Kanazawa, S., Asawa, Y., *et al.* Regenerative cartilage made by fusion of cartilage elements derived from chondrocyte sheets prepared in temperature-responsive culture dishes. J Hard Tissue Biology **23,** 101, 2014.
21. Mitani, G., Sato, M., Lee, J.I., *et al.* The properties of bioengineered chondrocyte sheets for cartilage regeneration. BMC Biotechnol **9,** 17, 2009.
22. Shimizu, T., Sekine, H., Yang, J., *et al.* Polysurgery of cell sheet grafts overcomes diffusion limits to produce thick, vascularized myocardial tissues. FASEB J **20,** 708, 2006.
23. Talab, S.S., Kajbafzadeh, A.-M., Elmi, A., *et al.* Bladder reconstruction using scaffold-less autologous smooth muscle cell sheet engineering: early histological outcomes for autoaugmentation cystoplasty. BJU Int **114,** 937, 2014.
24. Darling, E.M., Pritchett, P.E., Evans, B.A., Superfine, R., Zauscher, S., and Guilak, F. Mechanical properties and gene expression of chondrocytes on micropatterned substrates following dedifferentiation in monolayer. Cell Mol Bioeng **2,** 395, 2009.
25. Huang, B.J., Huey, D.J., Hu, J.C., and Athanasiou, K.A. Engineering biomechanically functional neocartilage derived from expanded articular chondrocytes through the manipulation of cell seeding density and dexamethasone concentration. J Tissue Eng Regen M **11,** 2323, 2016.
26. Makris, E.A., Responte, D.J., Paschos, N.K., Hu, J.C., and Athanasiou, K.A. Developing functional musculoskeletal tissues through hypoxia and lysyl oxidase-induced collagen cross-linking. Proc Natl Acad Sci U S A **111,** E4832–41, 2014.
27. Hu, J.C., and Athanasiou, K.A. A self-assembling process in articular cartilage tissue engineering. Tissue Eng **12,** 969, 2006.
28. Ofek, G., Revell, C.M., Hu, J.C., Allison, D.D., Grande-Allen, K.J., and Athanasiou, K.A. Matrix development in self-assembly of articular cartilage. PLoS One **3,** e2795, 2008.
29. Huey, D.J., Hu, J.C., and Athanasiou, K.A. Chondrogenically tuned expansion enhances the cartilaginous matrix-forming capabilities of primary, adult, leporine chondrocytes. Cell Transplant **22,** 331, 2013.
30. Huey, D.J., and Athanasiou, K.A. Alteration of the fibrocartilaginous nature of scaffoldless constructs formed from leporine meniscus cells and chondrocytes through manipulation of culture and processing conditions. Cells Tissues Organs **197,** 360, 2013.
31. Murphy, M.K., Huey, D.J., Hu, J.C., and Athanasiou, K.A. TGF-beta1, GDF-5, and BMP-2 stimulation induces chondrogenesis in expanded human articular chondrocytes and marrow-derived stromal cells. Stem Cells **33,** 762, 2015.
32. Kawakami, Y., Rodriguez-Leon, J., and Izpisua Belmonte, J.C. The role of TGFbetas and Sox9 during limb chondrogenesis. Curr Opin Cell Biol **18,** 723, 2006.
33. Elder, B.D., and Athanasiou, K.A. Systematic assessment of growth factor treatment on biochemical and biomechanical properties of engineered articular cartilage constructs. Osteoarthritis Cartilage **17,** 114, 2009.
34. Responte, D.J., Arzi, B., Natoli, R.M., Hu, J.C., and Athanasiou, K.A. Mechanisms underlying the synergistic

enhancement of self-assembled neocartilage treated with chondroitinase-ABC and TGF-beta1. Biomaterials **33,** 3187, 2012.
35. Kim, M., Song, K., Jin, E.J., and Sonn, J. Staurosporine and cytochalasin D induce chondrogenesis by regulation of actin dynamics in different way. Exp Mol Med **44,** 521, 2012.
36. Adkisson, H.D., Martin J.A., Amendola R.L., *et al.* The potential of human allogeneic juvenile chondrocytes for restoration of articular cartilage. Am J Sports Med **38,** 1324, 2010.
37. Smeriglio, P., Lai, J.H., Dhulipala, L., *et al.* Comparative potential of juvenile and adult human articular chondrocytes for cartilage tissue formation in three-dimensional biomimetic hydrogels. Tissue Eng A **21,** 147, 2015.
38. Barbero, A., Grogan, S., Schafer, D., Heberer, M., Mainil-Varlet, P., and Martin, I. Age related changes in human articular chondrocyte yield, proliferation and post-expansion chondrogenic capacity. Osteoarthritis Cartilage **12,** 476, 2004.
39. Adkisson, H.D., Milliman, C., Zhang, X., Mauch, K., Maziarz, R.T., and Streeter, P.R. Immune evasion by neocartilage-derived chondrocytes: implications for biologic repair of joint articular cartilage. Stem Cell Res **4,** 57, 2010.
40. Murphy, M.K., Huey, D.J., Reimer, A.J., Hu, J.C., and Athanasiou, K.A. Enhancing post-expansion chondrogenic potential of costochondral cells in self-assembled neocartilage. PLoS One **8,** e56983, 2013.
41. Woessner, J.F., Jr. The determination of hydroxyproline in tissue and protein samples containing small proportions of this imino acid. Arch Biochem Biophys **93,** 440, 1961.
42. Natoli, R.M., Skaalure, S., Bijlani, S., Chen, K.X., Hu, J., and Athanasiou, K.A. Intracellular Na(+) and Ca(2+) modulation increases the tensile properties of developing engineered articular cartilage. Arthritis Rheum **62,** 1097, 2010.
43. Allen, K.D., and Athanasiou, K.A. Viscoelastic characterization of the porcine temporomandibular joint disc under unconfined compression. J Biomech **39,** 312, 2006.
44. Nover, A.B., Jones, B.K., Yu, W.T., *et al.* A puzzle assembly strategy for fabrication of large engineered cartilage tissue constructs. J Biomech **49,** 668, 2016.
45. Loty, S., Forest, N., Boulekbache, H., and Sautier, J.M. Cytochalasin D induces changes in cell shape and promotes in vitro chondrogenesis: a morphological study. Biol Cell **83,** 149, 1995.
46. Saxena, V., Kim, M., Keah, N.M., *et al.* Anatomic mesenchymal stem cell-based engineered cartilage constructs for biologic total joint replacement. Tissue Eng A **22,** 386, 2016.

Address correspondence to:
Kyriacos A. Athanasiou, PhD, PE
Department of Biomedical Engineering
University of California Irvine
3120 Natural Sciences II
Irvine, CA 92697

E-mail: athens@uci.edu

Received: January 7, 2018
Accepted: May 10, 2018
Online Publication Date: June 27, 2018